J Physiol 591.5 (2013) pp 1385–1402

The Journal of Physiology

Sparing of muscle mass and function by passive loading in an experimental intensive care unit model

Guillaume Renaud[1], Monica Llano-Diez[1], Barbara Ravara[2], Luisa Gorza[2], Han-Zhong Feng[3], Jian-Ping Jin[3], Nicola Cacciani[1], Ann-Marie Gustafson[1], Julien Ochala[1], Rebeca Corpeno[1], Meishan Li[1], Yvette Hedström[1], G. Charles Ford[4], K. Sreekumaran Nair[4] and Lars Larsson[1]

[1] *Department of Neuroscience, Clinical Neurophysiology, Uppsala University, Sweden*
[2] *Department of Biomedical Sciences, University of Padova, Italy*
[3] *Department of Physiology, Wayne State University, Detroit, USA*
[4] *Division of Endocrinology, Endocrinology Research Unit, Mayo Clinic College of Medicine, Rochester, Minnesota, USA*

Key points

- Early physical mobilization of mechanically ventilated intensive care unit (ICU) patients can reduce the length of stay in the ICU and hospital and improve muscle strength and functional outcomes.
- A unique experimental rat ICU model has been used to study the effects and underlying mechanisms of unilateral passive mechanical loading on skeletal muscle size and function at durations varying between 6 h and 2 weeks.
- Passive mechanical loading attenuated the loss of muscle mass and force-generation capacity associated with the ICU intervention.
- The maintained muscle mass and function by passive loading is probably due to lower oxidative stress and a reduced loss of the molecular motor protein myosin.
- The beneficial effects of passive mechanical loading on muscle size and function strongly support the importance of early and intense physical therapy in immobilized ICU patients.

Abstract The response to mechanical stimuli, i.e. tensegrity, plays an important role in regulating cell physiological and pathophysiological function, and the mechanical silencing observed in intensive care unit (ICU) patients leads to a severe and specific muscle wasting condition. This study aims to unravel the underlying mechanisms and the effects of passive mechanical loading on skeletal muscle mass and function at the gene, protein and cellular levels. A unique experimental rat ICU model has been used allowing long-term (weeks) time-resolved analyses of the effects of standardized unilateral passive mechanical loading on skeletal muscle size and function and underlying mechanisms. Results show that passive mechanical loading alleviated the muscle wasting and the loss of force-generation associated with the ICU intervention, resulting in a doubling of the functional capacity of the loaded *versus* the unloaded muscles after a 2-week ICU intervention. We demonstrate that the improved maintenance of muscle mass and function is probably a consequence of a reduced oxidative stress revealed by lower levels of carbonylated proteins, and a reduced loss of the molecular motor protein myosin. A complex temporal gene expression pattern, delineated by microarray analysis, was observed with loading-induced changes in transcript levels of sarcomeric proteins, muscle developmental processes, stress response, extracellular matrix/cell adhesion proteins and metabolism. Thus, the results from this study show that passive mechanical loading alleviates the severe negative consequences on muscle size

*G. Renaud and M. Llano-Diez contributed equally to this paper

DOI: 10.1113/jphysiol.2012.248724

and function associated with the mechanical silencing in ICU patients, strongly supporting early and intense physical therapy in immobilized ICU patients.

(Received 19 November 2012; accepted after revision 21 December 2012; first published online 24 December 2012)
Corresponding author L. Larsson: Department of Neuroscience, Clinical Neurophysiology, University Hospital, Entrance 85, 3rd floor, SE-751 85 Uppsala, Sweden. Email: Lars.larsson@neuro.uu.se

Abbreviations AQM, acute quadriplegic myopathy; CSA, cross-sectional area; EDL, extensor digitorum longus; FSR, fractional protein synthesis rate; GO, Gene Ontology; ICU, intensive care unit; MyHC, myosin heavy chain; NMB, neuromuscular blockade; nNOS, neuronal nitric oxide synthase; SF, specific force; SQ, starting quantity; SL, sarcomere length; ST, specific tension; TA, tibialis anterior; TnI, troponin I; TnT, troponin T.

Introduction

The ability of the muscle cell to sense, process and respond to mechanical stimuli, i.e. *tensegrity*, is an important regulator of gene expression and protein synthesis and accordingly also an important regulator of physiological and pathophysiological function (Raskin *et al.* 2009). The complete loss of mechanical stimuli, i.e. mechanical silencing of skeletal muscle in mechanically ventilated, deeply sedated and/or pharmacologically paralysed intensive care unit (ICU) patients, results in a severe and specific muscle wasting condition. We have recently shown in time-resolved analyses using a unique experimental ICU model that the mechanical silencing *per se* is a dominating factor triggering the preferential myosin loss, atrophy and loss of specific force in fast- and slow-twitch muscles and muscle fibres (Ochala *et al.* 2011*b*). This phenotype is considered pathognomonic of the severe acquired myopathy in ICU patients most commonly named acute quadriplegic myopathy (AQM) or critical illness myopathy (CIM). AQM was for many years grouped with muscle paralysis of neurogenic origin, such as critical illness polyneuropathy and Guillain–Barré syndrome, due to misinterpretation of electrophysiological signals (Larsson, 2008). However, the muscle paralysis and severe muscle wasting in AQM has a primary myogenic origin. AQM was initially thought to be a rare event of limited clinical relevance, but it is now generally accepted to be the most frequent cause underlying acquired muscle paralysis among ICU patients, affecting about one-third of the general ICU patient population (De Jonghe *et al.* 2002; Cheung *et al.* 2006). This potentially lethal condition prolongs the recovery of critical care patients, thereby increasing the median ICU treatment costs 3-fold (Larsson, 2008). Furthermore, several studies have reported that critical illness survivors suffer from muscle weakness and fatigue, drastically impairing quality of life many years after hospital discharge (Leijten *et al.* 1995; Herridge *et al.* 2003, 2011; Cheung *et al.* 2006; Herridge, 2011).

Although the awareness of AQM has increased significantly in the past decade, many patients still fail to receive correct diagnosis and there is no specific treatment. However, early physical mobility therapy treatment has proven to be well tolerated and to have beneficial effects in ICU patients, such as increased strength, decreased length of hospital stay and hastened weaning from the ventilator (Ross, 1972; Burns & Jones, 1975; Nava, 1998; Martin *et al.* 2005; Morris *et al.* 2008; Burtin *et al.* 2009). Therefore, passive loading may diminish the severity of AQM, but the mechanisms underlying the specific effects of this intervention on skeletal muscle structure and function remain unknown.

This study aims to improve our understanding of the underlying mechanisms and the effects of passive mechanical loading on skeletal muscle size and function by using a unique experimental ICU model allowing analyses of the temporal sequence of changes in mechanically ventilated and pharmacologically paralysed animals. The effects of unilateral passive ankle joint flexions–extensions on distal hind limb muscle gene/protein expression, post-translational protein modifications (carbonylation), protein synthesis rate, protein degradation via the ubiquitin proteasome pathway and regulation of muscle contraction at the muscle cell level were studied at durations varying from 6 h to 14 days. It was hypothesized that passive loading will alleviate the muscle wasting and decreased force-generation capacity by reducing muscle proteolysis and the preferential myosin loss associated with AQM and mechanical silencing in the experimental ICU model. A significant positive temporal effect of passive mechanical loading on muscle fibre size and function was observed in response to loading-induced changes in gene/protein expression and post-translational protein modifications.

Methods

Animals

Fifteen sham operated controls and 46 anaesthetized and mechanically ventilated female Sprague–Dawley rats treated with α-cobratoxin for durations varying from 6 h to 14 days were included in this study. The experimental model has previously been described in detail (Dworkin & Dworkin, 1990, 2004). Briefly, all surgery and instrumentation were performed under sterile

techniques. (1) Precordial silver wire electrocardiogram (ECG) electrodes are implanted subcutaneously. (2) An aortic catheter (28-gauge Teflon) is inserted via the left carotid artery to record arterial blood pressure. (3) A 0.9 mm Renathane catheter is threaded into the left jugular vein to record venous blood pressure, and administer parental solutions. (4) Three subcutaneous electroencephalogram (EEG) needle electrodes are placed into the skull above the right and left temporal lobes, and a third reference electrode is placed in the neck region. (5) Temperature is measured by a vaginal thermistor and servo-regulated at 37°C. (6) A silicon cannula is inserted in the urethra to continuously record urine output. Animals were maintained in protein and fluid balance, i.e. (i) an intra-arterial solution (0.6 ml h^{-1}) consisting of 50 ml H_2O, 50 ml 0.5 N lactated Ringer solution, 1.25 g sodium oxacillin, 2.8 mg α-cobratoxin, 0.3 mg vitamin K (Synkavite) and 20 meq K^+ (as KCl); (ii) an intra-venous solution (0.6 ml h^{-1}) consisting of 50 ml H_2O, 50 ml 0.5 N lactated Ringer solution, 20% glucose (Baxter, Deerfield, IL, USA) and 1.25 g sodium oxacillin. The sham-operated control animals underwent the same interventions as the controls, but they were not pharmacologically paralysed with α-cobratoxin. That is, sham operated controls were anaesthetized (isoflurane), spontaneously breathing, given intra-arterial and intravenous solutions, and killed within 2 h after the initial anaesthesia and surgery.

During surgery or any possible irritating manipulation, the anaesthetic isoflurane level is at >1.5%, which maintains the following states: (1) the EEG is synchronized and dominated by high-voltage slow-wave activity; (2) mean arterial pressure (100 mmHg), heart rate (420 beats min^{-1}); and (3) no evident EEG, blood pressure or heart rate responses to surgical manipulation. Isoflurane is delivered into the inspiratory gas stream by a precision mass-flow controller. After the initial surgery, isoflurane is gradually lowered (over 1–2 days) and maintained at <0.5% during the remaining experimental period. Rats are ventilated through a per os coaxial tracheal cannula at 72 breaths min^{-1} with an inspiratory and expiratory ratio of 1:2 and a minute volume of 180–200 ml and gas concentrations of 49.5% O_2, 47% N_2 and 3% CO_2, delivered by a precision (volume drift <1% per week) volumetric respirator. Intermittent hyperinflations (six per hour at 15 cmH_2O), positive end-expiratory pressure (1.5 cmH_2O) and expiratory CO_2 monitoring are continuous. Neuromuscular blockade (NMB) was induced on the first day (100 μg I.V. α-cobrotoxin) and maintained by continuous infusion (250 μg day^{-1}, I.V.). Mechanical ventilation starts immediately after the NMB induction. The left leg of the animal was activated for 6 h at the shortest duration and 12 h day^{-1} at durations 12 h and longer throughout the experiment, using a mechanical lever arm that produced continuous passive maximal ankle joint flexions–extensions at a speed of 13.3 cycles min^{-1}.

Experiments were terminated at durations varying between 6 h and 14 days. Animals were killed by removing the heart during isoflurane anaesthesia during controlled mechanical ventilation. In no case did animals show any signs of infections or septicaemia. The Ethical Committee at Uppsala University approved all aspects of this study.

Muscles and muscle fibre membrane permeabilization

The tibialis anterior (TA), extensor digitorum longus (EDL), plantaris, gastrocnemius and soleus muscles were dissected from the loaded left leg and the unloaded right leg immediately after death. One half of the soleus and EDL muscles together with TA and gastrocnemius were quickly frozen in liquid propane cooled by liquid nitrogen, and stored at −160°C for further analyses. In the other halves of the soleus and EDL muscles, bundles of approximately 50 fibres were dissected from the muscles in relaxing solution at 4°C and tied to glass capillaries, stretched to about 110% of their resting slack length. The bundles were chemically skinned for 24 h in relaxing solution containing 50% (v/v) glycerol for 24 h at 4°C and were subsequently stored at −20°C (Larsson & Moss, 1993). All the bundles were cryo-protected within 1 week after skinning by transferring the bundles every 30 min to relax solution containing increasing concentrations of sucrose, i.e. 0, 0.5, 1.0, 1.5 and 2.0 M, and subsequently frozen in liquid propane chilled with liquid nitrogen (Frontera & Larsson, 1997). The frozen bundles were stored at −160°C pending use. One day before the experiments, a bundle was transferred to a 2.0 M sucrose solution for 30 min, subsequently incubated in solutions of decreasing sucrose concentration (1.5–0.5 M) and finally kept in a skinning solution at −20°C.

Single muscle fibre experimental procedure

On the day of an experiment, a fibre segment 1–2 mm long was left exposed to the experimental solution between connectors leading to a force transducer (model 400A; Aurora Scientific, Aurora, ON, Canada) and a lever arm system (model 308B; Aurora Scientific) (Moss, 1979). The apparatus was mounted on the stage of an inverted microscope (model IX70; Olympus). While the fibre segments were in relaxing solution, the sarcomere length was set to 2.65–2.75 μm by adjusting the overall segment length (Larsson & Moss, 1993). The diameter of the fibre segment between the connectors was measured through the microscope at a magnification of ×320 with an image analysis system prior to the mechanical experiments. Fibre depth was measured by recording the vertical displacement of the microscope nosepiece while focusing on the top and bottom surfaces of the fibre. The focusing control of the microscope was used as a micrometer.

Fibre cross-sectional area (CSA) was calculated from the diameter and depth, assuming an elliptical circumference, and was corrected for the 20% swelling that is known to occur during skinning (Moss, 1979).

Relaxing and activating solutions contained (in mM) 4 Mg-ATP, 1 free Mg^{2+}, 20 imidazole, 7 EGTA and 14.5 creatine phosphate, and KCl to adjust the ionic strength to 180 mM. The pH was adjusted to 7.0. The concentrations of free Ca^{2+} were 10^{-9} M (relaxing solution) and $10^{-4.5}$ M (activating solutions), expressed as *p*Ca values (i.e. $-\log[Ca^{2+}]$). Apparent stability constants for Ca^{2+}-EGTA were corrected for temperature (15°C) and ionic strength (180 mM). The computer program of Fabiato (1988) was used to calculate the concentrations of each metal, ligand and metal–ligand complex.

At 15°C, immediately preceding each activation, the fibre was immersed for 10–20 s in a solution with a reduced Ca^{2+}-EGTA buffering capacity. This solution is identical to the relaxing solution except that the EGTA concentration is reduced to 0.5 mM, which results in more rapid attainment of steady-state force during subsequent activation. Fibres were activated at *p*Ca of 4.5 and once steady tension was reached, various amplitudes of slack (ΔL) were rapidly introduced (within 1–2 ms) at one end of the fibre. For each amplitude of ΔL, the fibre was re-extended while relaxed to minimize non-uniformity of sarcomere length (SL). Maximum active tension (P_0) was calculated as the difference between the total tension in the activating solution (*p*Ca 4.5) and the resting tension measured in the same segment while in the relaxing solution. All contractile measurements were carried out at 15°C. The contractile recordings were accepted in subsequent analyses if SL during isometric tension development changed by more than 0.10 μm compared with SL while the fibre was relaxed or if force changed more than 10% from first to final activation (Moss, 1979). Specific tension (ST) was calculated as maximum tension (P_0) normalized to CSA.

After the mechanical measurements, each fibre was placed in urea buffer (120 g urea, 38 g thiourea, 70 ml H_2O, 25 g mixed bed resin, 2.89 g dithiothreitol, 1.51 g Trizma base, 7.5 g SDS, 0.004% bromophenol blue) in a plastic micro centrifuge tube and stored at −80°C for subsequent electrophoretic analyses.

SDS-PAGE and Western blotting

Myosin heavy chain (MyHC) isoform expression was determined by 6% SDS-PAGE prepared according to Larsson & Moss (1993). Total protein content was determined in 10 μm EDL and soleus muscle cross-sections dissolved in 100 μl 8 M urea buffer after centrifugation and heating (90°C for 2 min), using the NanoOrange® Protein Quantification Kit (Invitrogen, Carlsbad, CA, USA). The fluorescence of the samples was measured using a Plate Chameleon Multilabel Platereader (Hidex Oy, Turku, Finland) and the software MikroWin2000, version 4.33 (Microtek Laborsysteme GmbH, Overath, Germany). The fluorescence of the samples was related to a standard curve of bovine serum albumin (Invitrogen) at concentrations ranging from 10 to 0.1 μg ml^{-1}.

Actin and myosin contents were quantified on 12% SDS-PAGE. The acrylamide concentration was 4% (w/v) in the stacking gel and 12% in the running gel, and the gel matrix included 10% glycerol. Volumes of 5 μl of the samples were loaded together with 5 μl of the standard dilutions. The standard was prepared by pooling sections from control rat EDL and soleus muscles. The myofibrillar protein standards were prepared, assuming that actin and myosin contents were 12.5 and 25% of the total protein content, respectively. Linear actin and myosin curves were observed within the 5–200 μg ml^{-1} range, but the calibration curves were not parallel.

Electrophoresis was performed at 32.0 mA for 5 h with a Tris-glycine electrode buffer (pH 8.3) at 15°C (SE 600 vertical slab gel unit; Hoefer Scientific Instruments). The gels were stained using SimplyBlue SafeStain (Invitrogen) and subsequently scanned in a soft laser densitometer (Molecular Dynamics, Sunnyvale, CA, USA) with a high spatial resolution (50 μm pixel spacing) and 4096 optical density levels. The volume integration function was used to quantify the amount of protein on 12 and 6% gels (ImageQuant TL Software v. 3.3; Amersham Biosciences, Uppsala, Sweden).

Atrogin-1 and MuRF1 protein expressions were quantified in the soleus muscle by Western blotting as previously described (Ochala *et al.* 2011*b*). Membranes were incubated with Atrogin-1 (AP2041; ECM Biosciences, Versailles, KY, USA), MuRF1 (AF5366; R&D Systems, Minneapolis, MN, USA) and actin (sc-1616; Santa Cruz Biotechnology, Santa Cruz, CA, USA) primary antibodies. After incubation with the appropriate secondary antibodies conjugated with peroxidase NA934 (GE Healthcare, Little Chalfont, UK) or sc-2020 (Santa Cruz Biotechnology), blots were developed using an ECL Advance western blotting detection kit (RPN 2135; Amersham Biosciences) according to the manufacturer's instructions. The immunoblots were subsequently scanned in a soft laser densitometer (Molecular Dynamics). The signal intensities were quantified using the volume integration function (arbitrary unit) and normalized to actin content.

Troponin (Tn) isoform expression was measured in TA muscle samples homogenized in 20 volumes (w/v) of SDS-gel sample buffer containing 2% SDS, 10% glycerol, 50 mM Tris-base, 2% 2-mercaptoethanol, pH 8.8, using a high speed mechanical homogenizer (PRO Scientific, Inc.). The homogenized muscle samples were immediately heated at 80°C for 5 min, clarified

by high-speed centrifugation at top speed in a micro-centrifuge and stored at −80°C. For SDS-PAGE and Western blot analysis, the protein extracts were resolved on 14% Laemmli gel with an acrylamide/bisacrylamide ratio of 180:1. The protein bands were visualized by staining the gel with Coomassie Brilliant Blue R250. Duplicate gels were electrically transferred to blot nitrocellulose membranes. Tris-buffered saline (TBS) containing 1% bovine serum albumin (BSA) was used to block the nitrocellulose membranes at room temperature for 30 min. The membranes were then incubated with an anti-troponin I (TnI) monoclonal antibody (mAb) TnI-1 (Jin *et al.* 2001) or mAb T12 recognizing fast skeletal muscle troponin T (TnT) (Chong & Jin, 2009) diluted in TBS containing 0.1% BSA at 4°C overnight. After high-stringency washes with TBS containing 0.5% Triton X-100 and 0.05% SDS, the membranes were further incubated with alkaline phosphatase-conjugated goat anti-mouse IgG second antibody (Santa Cruz Biotechnology), washed again as above and developed in 5-bromo-4-chloro-3-indolylphosphate/nitro blue tetrazolium substrate solution.

Grp94 protein expression was quantified in the plantaris muscle by Western blotting, as previously described (Vitadello *et al.* 2003). Rabbit polyclonal anti-Grp94 antibody (SPA851; Stressgen, Victoria, BC, Canada) was used as primary antibody. After incubation with the appropriate secondary antibody conjugated with peroxidase (Santa Cruz Biotech., Heidelberg, Germany), blots were developed using an enhanced chemiluminescent detection system (ECL; GE Healthcare, Milan, Italy). Protein levels were quantified via measurement of optical density using the NIH Image J analysis software (Bethesda, MD, USA) and normalized to the densitometric value of the Ponceau red staining of the serum albumin band, which was chosen as a reference (Dalla Libera *et al.* 2009) instead of other muscle proteins, amounts of which might be affected by loading/unloading.

Protein carbonylation detection

To assess the formation of protein carbonyl groups, the OxyBlot protein oxidation detection kit (Chemicon, Chandler's Ford, UK) was used as previously described (Dalla Libera *et al.* 2009). In brief, about 10 muscle cryosections (12 μm) were solubilized at 4°C in 100 μl of 0.01% tetrafluoroacetic acid containing protease inhibitors, 5 mM EDTA and 2% β-mercaptoethanol. About 12 μg of total protein was then used for derivatization with Dinitrophenylhydrazine (DNPH) according to the manufacturer's detailed protocol and processed for Western blot analysis. A positive control included derivatization of 3 μg of oxidized BSA, whereas the negative control was performed with an equal amount of total protein reacted in the absence of DNPH. Levels of oxidized protein were quantified using the NIH ImageJ analysis software and normalized as described by Dalla Libera *et al.* (2009).

Fractional protein synthesis rate measurements using [ring-$^{13}C_6$]phenylalanine as tracer

An I.V. bolus dose of [ring-$^{13}C_6$]phenylalanine (15 μg g^{-1} body weight) was given 15 min prior to the animals being killed. Immediately after death, the gastrocnemius muscle was removed from the left and right hindlimb and split into a medial and lateral deep red and superficial white portion and frozen in liquid propane chilled by liquid nitrogen. Tissue fluid and mixed gastrocnemius muscle proteins were isolated according to the method of Ljungqvist *et al.* (1997). The mixed muscle protein precipitate from the isolation was hydrolysed by heating with 6 M HCl overnight at 110°C. Both tissue fluid and hydrolysed mixed gastrocnemius muscle amino acids were purified using a BioRad AG-50 × 8 ion exchange resin prior to mass spectrometry analysis.

Tissue fluid. The level of enrichment of [ring-$^{13}C_6$]phenylalanine in tissue fluid was analysed using ThermoFisher Quantum gas chromatography tandem mass spectrometry (GC/MS/MS) (San Jose, CA, USA). The heptafluorobutyryl isobutyl ester derivative was prepared as described by Ford *et al.* (1985) and the amino acids were measured under negative ion chemical ionisation conditions using isobutane as reactant gas. The [M-HF]$^-$ fragments reflecting the m0 and m+6 species were monitored (m/z transitions 397→377 and 403→383, respectively) and the enrichment of the label was measured against a calibration curve prepared from known amounts of labelled and unlabelled phenylalanine (range 0–30%).

Mixed gastrocnemius muscle proteins. The level of enrichment of [ring-$^{13}C_6$]phenylalanine derived from hydrolysed mixed muscle proteins were analysed using a ThermoFisher DeltaPlus Isotope Ratio mass spectrometer (IR/MS) (Bremen, Germany) fitted with an on-line gas chromatograph with oxidation and reduction furnaces as previously described (Balagopal *et al.* 1996). The amino acids were derivatized to their trimethyl acetyl, methyl esters according to the method of Metges *et al.* (1996). Any amino acid eluting from the gas chromatograph is converted to CO_2 and N_2 prior to entry into the IR/MS. The amino acids were derivatized to their trimethyl acetyl, methyl esters according to the method of Metges *et al.* (1996). Enrichment of the tracer was measured by monitoring the ratio of ^{13}C to $^{12}CO_2$ in the IR/MS and again referenced to a calibration curve (0–0.1%).

In accordance with our previous study, there was no significant difference in fractional protein synthesis rate (FSR) between the medial and lateral portions of the gastrocnemius muscle independent of depth, but FSR was significantly higher in the deep than in the superficial portions (Ochala *et al.* 2011*b*). Therefore, FSR data from medial and lateral portions of the gastrocnemius muscle have been pooled, but analysed separately according to depth.

Total RNA isolation and quantification

Total RNA was extracted from frozen gastrocnemius muscle (proximal part) tissue (10–30 mg) using a Qiagen RNeasy Mini Kit (Qiagen, Inc., Valencia, CA, USA). Muscle tissue was homogenized using a motor homogenizer (Eurostar Digital; IKAWerke, Staufen, Germany). QIAshredder columns (Qiagen) were used to disrupt DNA. Total RNA was eluted from RNeasy Mini columns with 30 μl of RNase-free water. RNA concentrations were then quantified using the fluorescent nucleic acid stain Ribogreen (Molecular Probes, Eugene, OR, USA), on a Chameleon PLC IIs (Hidex) fluorescence spectrophotometer.

Expression profiling

Three micrograms of total RNA from the proximal gastrocnemius muscle samples was extracted and processed to generate biotin-labelled cRNA as previously described (Chen *et al.* 2000). Each sample was then hybridized to an Affymetrix Rat Gene 1.0 ST Array. The data discussed here have been deposited in the NCBI Gene Expression Omnibus (GEO) and are accessible through GEO Series accession number GSE37944.

Microarray data normalization and analyses

Subsequent analyses of the gene expression data were carried out in the freely available statistical computing language R using packages available from the Bioconductor project. The raw data were normalized using the robust multi-array average (Irizarry *et al.* 2003) background-adjusted, normalized and log-transformed summarized values first suggested by Li & Wong (2001). To search for the differentially expressed genes between the samples from the different days, an empirical Bayes-moderated *t* test was applied (Smyth, 2004), using the 'limma' package. A linear model was fitted to the data, unloaded *versus* loaded at the following durations: 6 h to 4 days, 5–8 days and 9–14 days. Probe sets with a minimum fold change of ± 1.5 at least in one time point were included in further analyses. Each differentially expressed gene was flagged by Gene Ontology (GO) classification, including molecular function, biological process and cellular component. The transcripts contained in each group at the different time durations were subjected to improved annotation using the DAVID web-based functional annotation tool (Huang da *et al.* 2007). Some of the functional categories were combined and some categorization was done manually, to improve the interpretative value of the data.

Quantitative (q)RT-PCR

qRT-PCR was used to quantify the mRNA levels for rat *Myh2* (MyHC-IIa), *Myh7* (MyHC-slow), *atrogin-1/Fbox32* and *Murf1/Trim63* (GenBank: L13606, GenBank: X15939, GenBank: AY059628, GenBank: AY059627, respectively). One hundred nanograms of total RNA from proximal gastrocnemius muscle samples was reverse transcribed to cDNA using Qscript cDNA supermix (Quanta Biosciences, Gaithersburg, MD, USA). cDNA was amplified in triplicate using an MyiQ single colour real time PCR detection system (Bio-Rad Laboratories, Inc., Hercules, CA, USA). RT-PCR was performed as described previously (Norman *et al.* 2006; Nordquist *et al.* 2007). PCR products were run on 2% agarose gels to ensure that primer–dimer formation was not occurring. Taqman primers and probes were designed using the software Primer Express (Applied Biosystems, Foster City, CA, USA). Primer and probe sequences have been published elsewhere (Norman *et al.* 2006; Nordquist *et al.* 2007) and were purchased from Thermo Electron (Ulm, Germany). All primers and probes were purified by high-performance liquid chromatography. Threshold cycle (C_t) data obtained from running real-time RT-PCR was related to a standard curve to obtain the starting quantity (SQ) of the template cDNA, and the values were normalized against 18S rRNA (GenBank: AF102857).

Statistics

Means and standard deviations were calculated according to standard procedures. One- and two-way analyses of variance (ANOVA) and the Tukey *post hoc* test were used when comparing multiple groups and $P < 0.05$ was considered statistically significant.

Results

Body and muscle weights

Body and muscle weights did not differ significantly between controls and the 0.25–4 day group, but declined at the longer durations (Table 1). A sparing of muscle weight on the loaded side was observed early during the intervention, but became statistically significant at the

Table 1. Body weight before and after intervention, and tibialis anterior, extensor digitorum longus, gastrocnemius, soleus and plantaris muscle weights on the left and right sides for sham-operated control animals and animals exposed to the ICU intervention for 0.25–4 days, 5–8 days and 9–14 days

	BW (g)		TA (mg)		EDL (mg)		Gast (mg)		SOL (mg)		PL (mg)	
Duration	*pre*	*post*	*left*	*right*	*left*	*right*	*left*	*right*	*left*	*right*	*left*	*right*
Controls[1] (*n*=12)	311±26	311±26	555±47	560±56	144±10	144±11	1652±213	1658±133	126±12	121±20	299±64	323±28
0.25–4 days[2] (*n*=20)	307±18	307±21	534±53	519±44*	132±11	133±17	1545±111	1503±116*	119±19	116±18	286±27	279±31
5–8 days[3] (*n*=3)	281±42^{1,2}	235±37^{1,2,*}	430±75^{1,2}	383±44^{1,2}	105±19^{1,2}	99±15^{1,2,**}	999±148^{1,2}	969±163^{1,2}	87±16^{1,2}	79±12^{1,2}	215±22^{1,2}	205±30^{1,2}
9–14 days[4] (*n*=8)	301±47^{1,2}	199±33^{1,2,**}	357±86^{1,2}	316±96^{1,2,*}	98±23^{1,2}	81±20^{1,2,***}	843±264^{1,2}	770±232^{1,2,**}	93±21^{1,2}	68±18^{1,2,**}	163±35^{1,2}	146±35^{1,2,***}
P	<0.001		<0.001		<0.001		<0.001		0.001		0.001	

BW, body weight; TA, tibialis anterior; EDL, extensor digitorum longus; GAST, gastrocnemius; SOL, soleus; PL, plantaris. Significant differences between groups are presented as superscripts and between loaded and unloaded side as asterisks ($^{*}P < 0.05$, $^{**}P < 0.01$, $^{***}P < 0.001$). Values are means ± SD.

longest durations and affected all muscles irrespective of type, i.e. fast-twitch, slow-twitch or mixed (Table 1). The average relative differences in muscle weights between the loaded and unloaded side were therefore pooled. According to one-way ANOVA, the difference in pooled muscle weight between loaded and unloaded side increased with increasing duration ($P < 0.001$), i.e. a stronger effect was observed in the 9–14 day group than in the 0.25–4 and 5–8 day groups (Fig. 1).

Contractile properties and size at the single muscle fibre level

Detailed analyses of CSA and force generation capacity (maximum force normalized to muscle fibre CSA, i.e. specific force (SF)) at the single muscle fibre level were restricted to the longest duration with the most pronounced effect on muscle size. A total of 160 muscle fibres from the fast-twitch EDL ($n = 80$) and the slow-twitch soleus ($n = 80$) fulfilled the criteria for acceptance (see Methods), and were included in the analyses. Muscle fibre CSA and SF were measured in both the loaded and the unloaded leg in each animal.

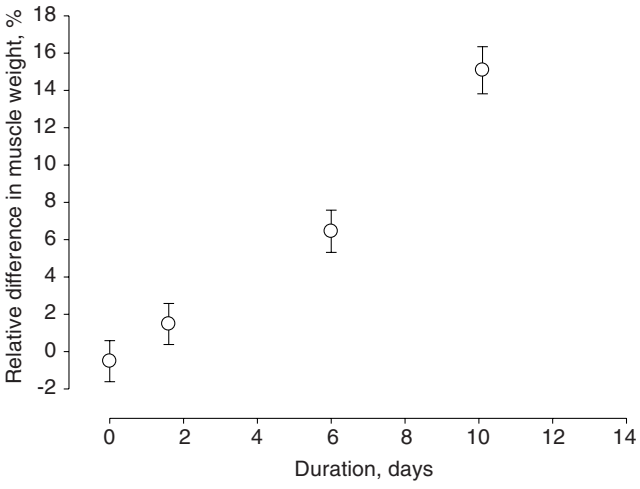

Figure 1. Relative difference in average muscle weights of gastrocnemius, plantaris, soleus, EDL and tibialis anterior muscles on the loaded versus the unloaded side
Positive values indicate larger muscle mass on the loaded side. Values are means ± SD.

In all animals, CSA and SF were higher ($P < 0.05$–0.001) on the loaded *versus* the unloaded side in both EDL and soleus fibres (Fig. 2). The average decline ($P < 0.05$) in passively loaded EDL and soleus muscle fibre CSA was 33 ± 4 and 18 ± 3%, respectively, compared with controls. The corresponding decline ($P < 0.05$) was 52 ± 3 and 43 ± 2% in the unloaded EDL and soleus, respectively. Thus, a stronger atrophy response was observed on the unloaded than on the loaded side according to two-way ANOVA analyses ($P < 0.05$–0.001, Fig. 2*C* and *D*). SF in passively loaded EDL and soleus fibres ($P < 0.05$) was 32 ± 4 and 26 ± 3% lower than in control EDL and soleus fibres, respectively. The corresponding decline ($P < 0.05$) was 60 ± 2 and 52 ± 2% in the unloaded EDL and soleus fibres, respectively, representing a significantly lower (two-way ANOVA, $P < 0.05$–0.001) force generation capacity on the unloaded side irrespective of muscle type (Fig. 2*A* and *B*). Thus, the aggregate effects of both fibre size and SF on overall muscle function indicate an approximate 46 and 53% residual function in the EDL and soleus, respectively, on the loaded side compared with 20 and 27% in the EDL and soleus, respectively, on the unloaded side. Thus, the passive loading intervention resulted in an approximate doubling of the functional capacity of both fast- and slow-twitch limb muscles.

Gene expression

Of the 26,208 probe sets, 245 genes showed a minimum ± 1.5-fold expression change on the loaded *versus* the unloaded side in at least one of the different passive loading durations (0.25–4, 5–8 and 9–14 days). A total of 33, 138 and 141 probe sets fulfilled the cut-off criteria in the 0.25–4, 5–8 and 9–14 day groups, respectively.

The 245 expressed genes were assigned functional annotations based on GO information. These genes were classified into enriched functional-related groups in order to unravel the most relevant functional categories and biological networks activated or suppressed in response to mechanical loading at the different durations. Complete

information (fold change, GO terms and functional classification) for all 245 probe sets is listed separately (Additional file 1).

0.25–4 day group. Only a small number of up- and down-regulated genes were observed in this group. Of the seven up-regulated genes, two were coding growth factors (connective tissue growth factor (*Ctgf*), and heparin-binding EGF-like growth factor (*Hbegf*)). Among the down-regulated genes, 26 genes coding sarcomeric proteins were observed, such as contractile proteins (*β*/slow myosin heavy chain isoform (*Myh7*) and a regulatory myosin light chain 2 (*Myl2*)), regulatory proteins (troponin I, T and C (*Tnni1*, *Tnnt1*, and *Tnnc1*)) and a structural sarcomeric protein (myozenin 2 (*Myoz2*)). The muscle-specific transcription factor myogenin (*Myog*) was also down-regulated.

5–8 day group. Up-regulation in response to loading was observed in 67 genes separated into three different groups. (i) Sarcomeric: in contrast to the shortest duration (0.25–4 days), an up-regulation of both fast and slow myosin heavy chain (*Myh7*, *Myh2*), myosin light chain (*Myl2*), structural (*Myoz2)* and regulatory protein (*Tnnt1*, *Tnnc1*) isoform genes were observed; (ii) muscle development/growth: follistatin m(*Fst*), and the muscle-specific caveolin-3 (*Cav3*) were up-regulated; and (iii) extracellular matrix/cell adhesion: chondroadherin (*Chad*), thrombospondin 4 (*Thbs4*), lysyl oxidase (*Lox*), asporin (*Aspn*) and biglycan (*Bgn*) were up-regulated.

A total of 71 down-regulated genes were observed in the 5–8 day group in response to loading, i.e. genes involved in: (i) the oxidative stress response (e.g. anti-oxidants aldehyde oxidase 1 (*Aox1*), metallothioneins 2a and 1a (*Mt2a* and *Mt1a*) and glutathione S-transferase (GST)); (ii) chaperone coding genes (heat shock protein 5 (*Hspa5*), heat shock protein 90 kDa beta member 1 (*Hsp90b1*/*Grp94*), AHA1 activator of heat shock protein ATPase homolog 2, yeast (*Ahsa2*) and protein disulfide isomerase family A, member 6 (*Pdia6*));

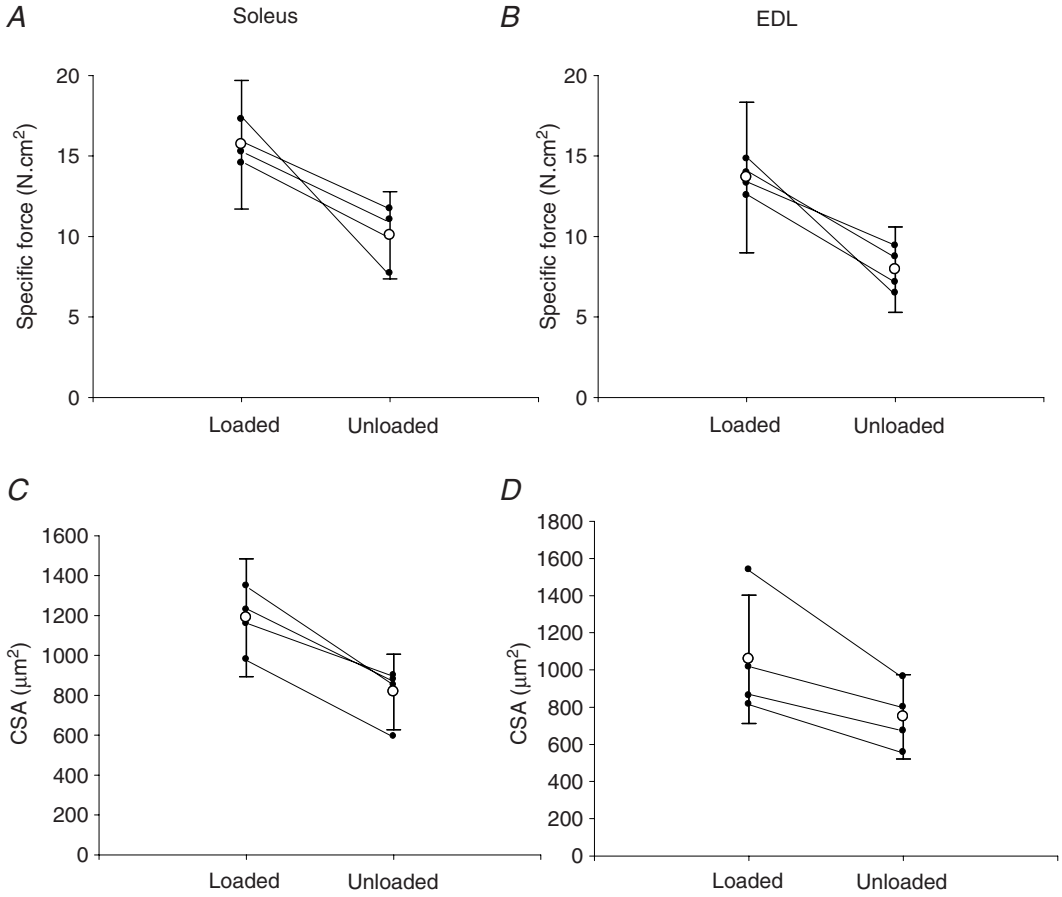

Figure 2. Muscle fibre specific force and cross-sectional area in the loaded and unloaded leg in animals exposed to unilateral loading, mechanical ventilation and neuromuscular blockade
A–D, individual (filled circles) and pooled (open circles) soleus and EDL single muscle fibre specific force (*A* and *B*) and cross-sectional area (CSA) (*C* and *D*) in the loaded (left) and unloaded leg (right) in animals exposed to unilateral loading, mechanical ventilation and neuromuscular blockade for 9–14 days. Values are means ± SD.

(iii) hypoxia response genes (hypoxia up-regulated 1 (*Hyou1*) and transferrin receptor (*Tfcr*)); and (iv) genes involved in metabolism. Other selected down-regulated genes were neuronal nitric oxide synthase 1 (*Nos1*), TGFβ-induced factor homeobox 1 (*Tgif1*) and the cystatin F (leukocystatin) (*Cst7*), a cathepsin inhibitor.

9–14 day group. There was a maintained up-regulation of 76 genes coding sarcomeric proteins, i.e. *Myh7*, *Myl2*, *Myl3*, *Myh2*, *Myoz2*, *Tnni1*, *Tnnt1* and *Tnnc*. The ankyrin repeat domain 2 (*Ankrd2*), involved in the stretch response, was up-regulated together with muscle development/growth genes, i.e. *Fst*, and myogenic factor 5 (*Myf5*) and some extracellular matrix/cell adhesion genes such as collagen type VIII, alpha 1 (*Col8a1*), elastin (*Eln*), versican (*Vcan*), fibrillin 1 (*Fbn1*), *Chad*, *Thbs4*, *Lox*, *Aspn* and *Bgn*. Insulin-like growth factor II (*Igf-2*) was up-regulated in response to loading at the longest observation period.

A total of 65 genes were down-regulated, such as immune response, antioxidant (*Aox1* and GST), chaperone coding (e.g. heat shock protein 90, alpha, cytosolic, class A, member 1 (*Hsp90aa1*), heat shock 105 kDa/110 kDa protein 1 (*Hsph1*) and clusterin (*Clu*)) and several metabolism-related genes. A graphical summary of the most relevant up- and down-regulated functional categories in response to passive mechanical loading at the different time points is shown in Fig. 3.

To confirm the array data, myosin heavy chain genes (*Myh2* and *Myh7*) and the atrogenes *Murf1*/*Trim63* and *atrogin-1*/*Fbox32* were selected. Similar fold-change patterns were observed between the arrays and qRT-PCR (see Additional file 2), validating the microarray results.

Protein synthesis rate

FSR was measured in the deep oxidative and superficial glycolytic region of the gastrocnemius muscle in 15 experimental and 9 control animals (FSR results on the unloaded side have been presented in 21 of these 24 animals in a previous study (Ochala *et al.* 2011*b*)). FSR was significantly higher ($P < 0.001$) in the deep than in the superficial portions independent of loading condition or the duration of the ICU condition (0 h to 14 days). On the unloaded side, a significant increase in synthesis rate was observed after 9–14 days exposure to the ICU intervention compared with controls and the 0.25–4 day group in both the deep oxidative ($P < 0.001$) and the superficial ($P < 0.001$) glycolytic regions of the muscle according to two-way-ANOVA. On the loaded side, on the other hand, no significant difference was observed in FSR at the different durations of the ICU intervention

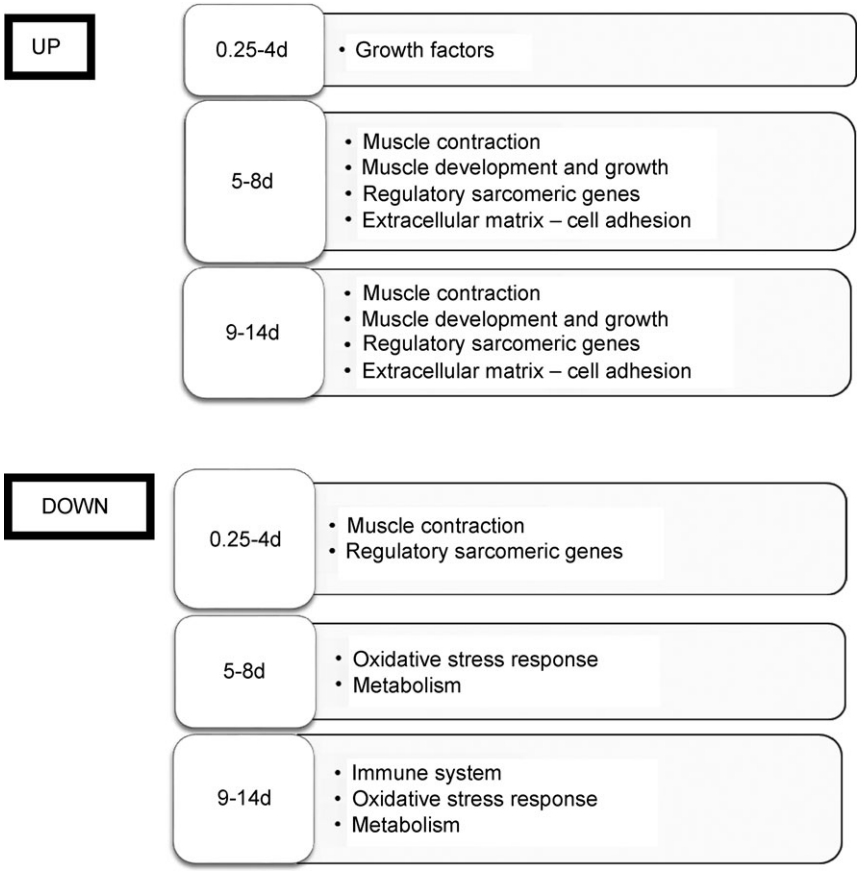

Figure 3. Graphical summary of the most relevant up- and down-regulated gene functional categories due to mechanical loading compared to the unloaded muscle at the different time points

in the oxidative and glycolytic regions of the muscle. Furthermore, FSR was higher ($P < 0.01$) in the unloaded than in the loaded leg in both the deep oxidative and the superficial deep region of the muscle at the longest duration of the ICU intervention, but no difference was observed at the other durations (Fig. 4). Thus, loading alleviated the immobilization-induced increase in FSR observed on the unloaded side as well as reported in ICU patients in response to long-term immobilization (Essen *et al.* 1998; Gamrin *et al.* 2000; Tjader *et al.* 2004)

Contractile and regulatory protein expression

Myofibrillar protein contents from the slow-twitch soleus and the fast-twitch EDL were separated and quantified together with myosin and actin standards on Coomassie-stained 12% SDS-PAGE and normalized to the total protein content loaded on the gel. Similar myosin protein contents were observed in controls and the 0.25–4 day group on both sides, but decreased progressively at the two longer durations in both the soleus and EDL according to two-way ANOVA ($P < 0.05$, Fig. 5*A* and *B*). In the slow-twitch soleus, passive loading reduced the myosin loss by 36 and 55% in the 5–8 and 9–14 day groups, respectively. In the EDL, a 16% reduction in myosin loss was observed in response to loading in the 9–14 day group, but failed to reach the level of statistical significance ($P = 0.10$, Fig. 5*A*). Actin protein content, on the other hand, was not affected by either loading or unloading during the whole experimental period in both the EDL and soleus (Fig. 5*A* and *B*).

An identical pattern and level of alternatively spliced fast TnT and MyHC isoform expression were found in the loading and unloading groups. No type I MyHC was detected in the fast-twitch TA muscle in either group, confirming the maintained fast fibre type profile (Fig. 6).

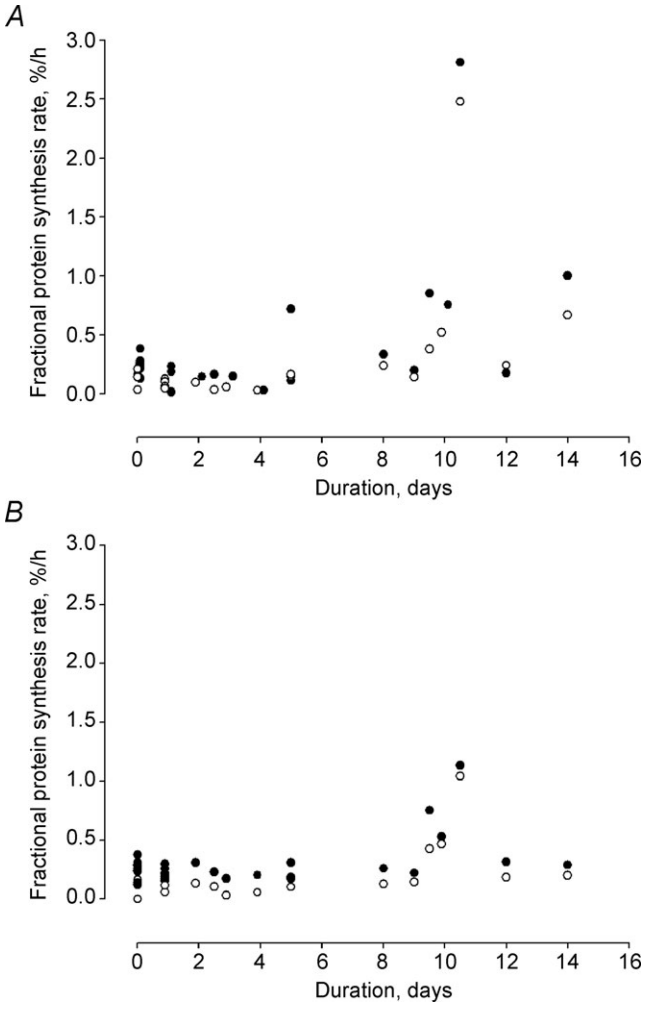

Figure 4. Fractional protein synthesis rate in the gastrocnemius muscle on the unloaded and loaded side and in controls
A and *B*, fractional protein synthesis rate in the deep (closed circles) and superficial region (open circles) of the gastrocnemius muscle on the unloaded (*A*) and loaded (*B*) side at durations varying from 6 h to 14 days and in controls.

Protein modifications

Oxidative stress was assessed in the plantaris muscle by quantifying the formation of carbonyl groups in amino acid side chains. Protein carbonylation levels were unchanged during the initial 6 h to 8 days of the ICU intervention irrespective of loading condition, but an increased ($P < 0.05$) protein oxidation was observed after longer exposure to the ICU intervention (9–14 days) on the unloaded side compared with controls (Fig. 7*A*). On the loaded side, carbonylation levels were not different from controls in the 9–14 d group according to two-way ANOVA.

Based on array data, stress-protein response was investigated on plantaris muscle by quantifying protein levels of Grp94, the product of the *Hsp90B1* gene. A decline ($P < 0.05$) in Grp94 protein content was observed in the 0.25–4 day group on both the loaded and the unloaded side compared with controls (Fig. 7*B*). In the unloaded leg, Grp94 protein content returned to control levels after 5–8 and 9–14 days of mechanical ventilation and NMB. On the loaded side, the Grp94 chaperone content was 92% higher ($P < 0.05$) in the 5–8 day group than in the control group and returned to control values in the 9–14 day group (Fig. 7*B*).

The ubiquitin proteasome degradation pathway

We have previously shown that the preferential myosin loss associated with the experimental ICU condition was preceded by an up-regulation of the ubiquitin proteasome

pathway while the lysosomal and calcium-activated pathways were activated at a later stage when the myosin loss was already established (Ochala *et al.* 2011*b*). We have therefore focused our interest on the effects of passive mechanical loading on Atrogin-1 and MuRF1 content (Fig. 8) in the soleus muscle. In accordance with our previous observations, Atrogin-1 content remained unchanged during the experimental period while MuRF1 content was increased in the 6 h to 4 day group compared with controls and remained elevated throughout the experimental period (two-way ANOVA, $P < 0.01$). In addition, MuRF1 protein content was lower on the loaded

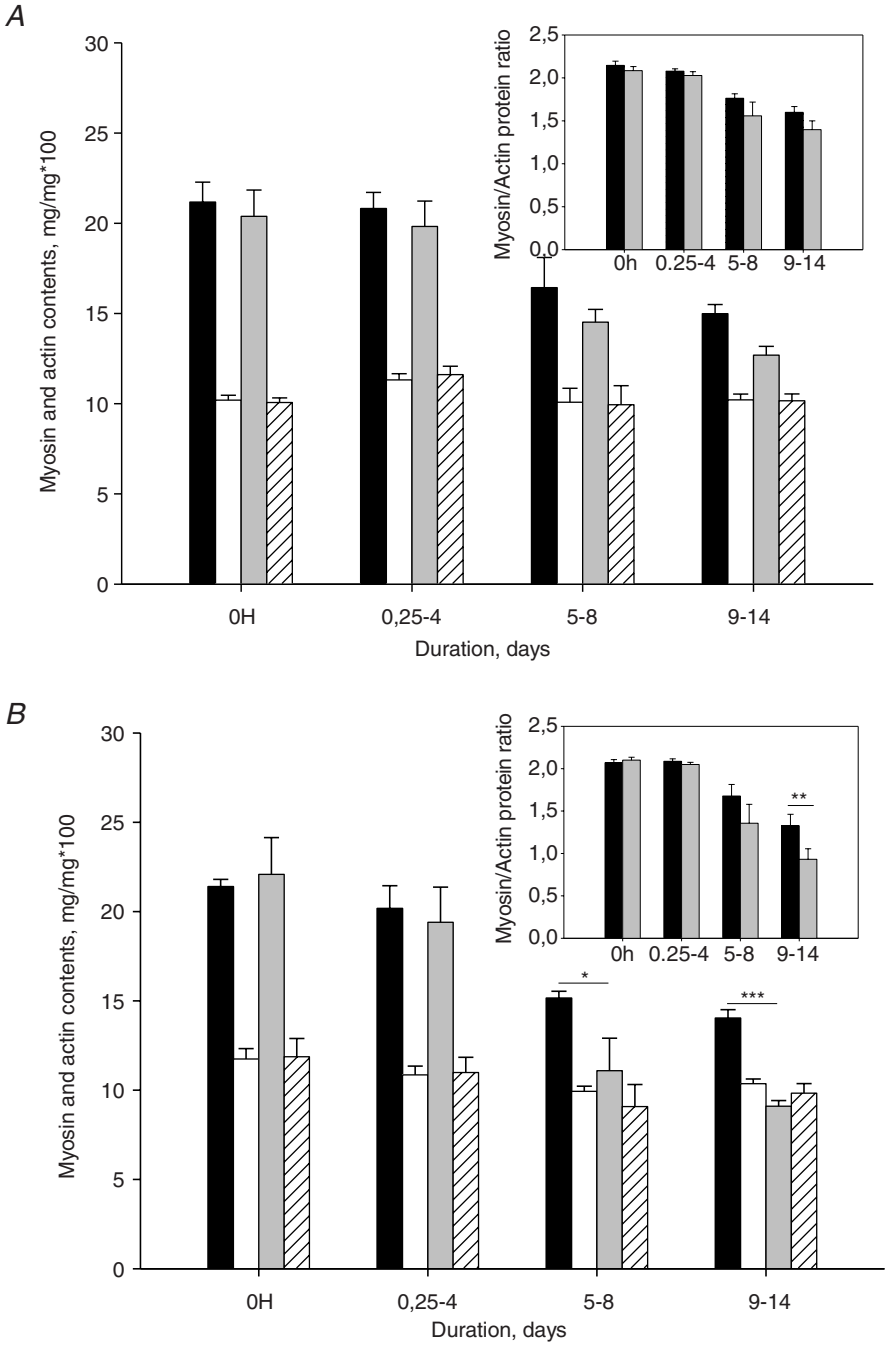

Figure 5. Myosin in the loaded and unloaded side and actin in the loaded and unloaded side
A and *B*, myosin in the loaded (black) and unloaded (grey) side and actin in the loaded (white) and unloaded (white striped) side contents normalized to total protein content in the EDL (*A*) and soleus (*B*). Myosin/actin ratios are shown in inset *A* for the EDL and *B* for the soleus in the loaded (black) and unloaded (grey) side. Asterisks indicate a significant difference between loaded and unloaded side: $^{*}P < 0.05$, $^{**}P < 0.002$, $^{***}P < 0.001$. Values are means + SD.

than the unloaded side after 5–8 days of mechanical loading (two-way ANOVA, $P < 0.01$; Fig. 8).

Discussion

There is an increasing interest in the effects of early physical activity on muscle function in mechanically ventilated and bed-ridden ICU patients, in part triggered by the escalating costs related to prolonged ICU treatment (Nava, 1998; Martin *et al.* 2005). Positive effects of early ambulation on wellbeing, muscle strength as well as hastened weaning from the ventilator have been reported in ICU patients (Ross, 1972; Burns & Jones, 1975), but the molecular and cellular mechanisms underlying the beneficial effects remain unclear. In this study, a unique experimental rat ICU model has been used allowing long-term (weeks) time-resolved analyses of the effects of standardized unilateral passive mechanical loading on skeletal muscle size and function and underlying mechanisms at the gene, protein and cellular levels. The major findings from this study on the effects of passive mechanical loading are: (1) a significant muscle sparing effect and an improved force generation capacity at the single muscle fibre level; (2) a reduced loss of the molecular motor protein myosin in the slow-twitch soleus; (3) a reduced oxidative stress revealed by lower levels of protein carbonylation; and (4) a complex temporal gene expression pattern delineated by microarray analysis with significant loading-induced changes in transcript levels of sarcomeric proteins, muscle developmental processes, stress response (oxidative and heat shock proteins), ECM/cell adhesion proteins and metabolism.

Regulation of muscle size and muscle contraction

Mechanical loading reduced the loss in both muscle mass and specific force associated with ICU intervention in both fast- and slow-twitch muscles, resulting in an approximate doubling of the functional capacity in loaded *versus* unloaded muscles after 2 weeks of mechanical loading 12 h per day. Furthermore, the relative muscle sparing effect increased with the duration of the mechanical loading and was paralleled by similar transcriptional up-regulation of contractile proteins: type I and IIa MyHCs (*Myh7*, *Myh2*), MyLCs (*Myl2*, *Myl3*), troponins (*Tnni1*, *Tnnt1* and *Tnnc*) and *Myoz2* were up-regulated from 5 to 14 days. The loading-induced changes in transcriptional regulation of contractile proteins resulted in a reduced preferential myosin loss in the slow-twitch soleus muscle and a similar trend, albeit not statistically significant, in the fast-twitch muscle with a slower protein turnover rate than in slow-twitch muscles (Lewis *et al.* 1984). Thus, these results collectively demonstrate a loading effect on protein synthesis, but the mechanisms underlying the improved muscle size and function in response to loading are more complex, also involving muscle protein degradation and regeneration pathways. The lower activation of MuRF1 in response to loading supports a reduced activation of the ubiquitin–proteasome proteolytic pathway, i.e. the

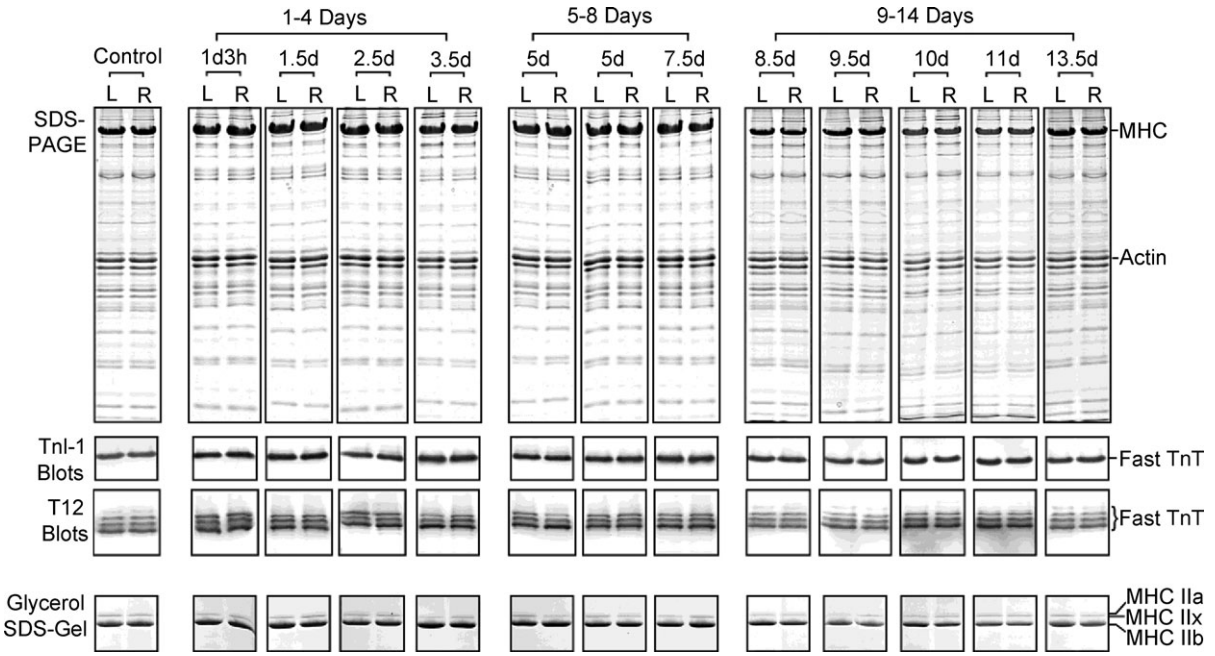

Figure 6. Western blots of tibialis anterior muscles treated with loading or unloading conditions
Tibialis anterior (TA) muscles treated with loading (L, left leg) or unloading (R, right leg) conditions were examined by Western blotting using mAb T12 recognizing fast TnT or TnI-1 recognizing all TnI isoforms.

pathway closely involved in the preferential myosin loss in response to ICU intervention.

Immobilization-induced post-translational protein modifications are critical for both protein function and triggering protein degradation. The beneficial effects of passive mechanical loading on the oxidative stress response and the lower levels of carbonylated proteins may accordingly reduce myosin degradation on the loaded side as carbonylated proteins are more prone to proteolysis (Grune *et al.* 2003). In ICU patients, several studies have shown that total FSR is highly variable (Essen *et al.* 1998; Gamrin *et al.* 2000; Tjader *et al.* 2004), although heterogeneity in the underlying disease, pharmacological treatment and age among the patients might partly account for such discrepancy. We have previously reported an increased FSR in response to long-term immobilization in the experimental ICU model (Ochala *et al.* 2011*b*) concomitant with a dramatic down-regulation of contractile proteins and up-regulation of the major proteolytic pathways (Ochala *et al.* 2011*b*). The increase in FSR of muscle proteins occurred while the concentrations of contractile proteins decreased, indicating a high degradation rate of proteins in the ICU environment. Increased protein degradation rates are usually associated with increased protein synthesis but when degradation exceeds synthesis a net protein loss causes muscle wastage. It appears that the mechanical loading normalized this accelerated protein degradation. Reduced oxidative stress and associated reduction in oxidative damage to proteins during passive mechanical loading may be responsible for reduced protein degradation. In this experiment, we observed an alleviation of the immobilization-induced increase in FSR in response to passive mechanical loading.

An up-regulation of genes controlling muscle development and skeletal muscle mass was observed;

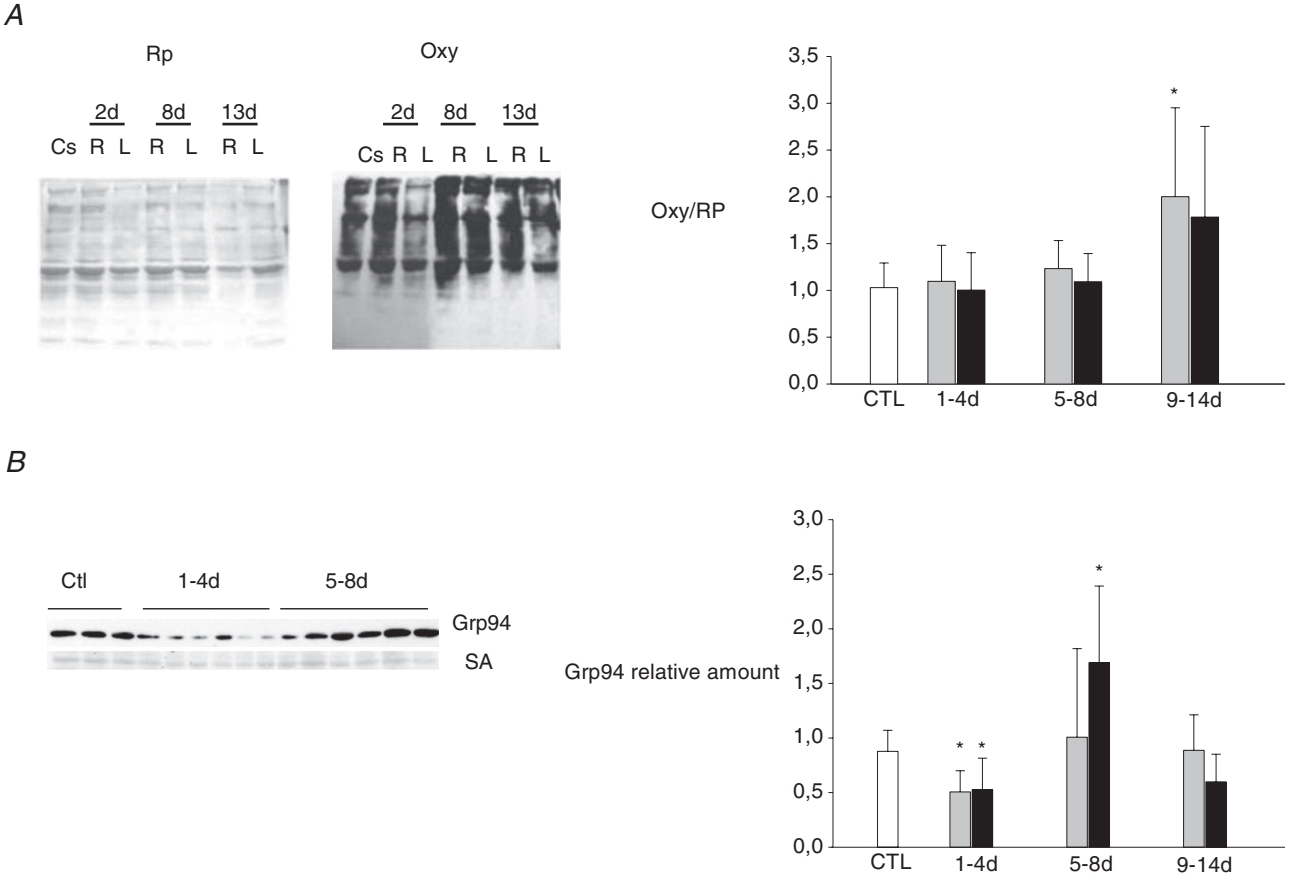

Figure 7. Grp94 protein levels as well as protein carbonylation in response to unilateral mechanical loading in rats exposed to NMB and mechanical ventilation at durations varying from 0 h (controls) to 14 days in the plantaris muscle

A, Red Ponceau (RP) stainings and Oxyblots (Oxy) from 2, 8 and 13 days in both the loaded and the unloaded side. Bar graph of Oxy/RP in controls (white), unloaded side (grey) and loaded side (black). Values are means + SD. $^*P < 0.05$ (significant difference compared with controls). *B*, Grp94 expression was analysed by Western blotting of samples from control, and 1, 2, 4, 5 and 8 days in both loaded and unloaded side. Bar graph shows the relative amount of Grp94 normalized to serum albumin (SA) levels in controls (white), unloaded side (grey) and loaded side (black).

for example, the myogenic factor *Myf5*, which plays an important role in satellite cell activation during embryogenesis and in adult muscles (Grefte *et al.* 2007), was up-regulated from 9 to 14 days. Passive mechanical loading also induced an up-regulation of *Ankrd2* from 9 to 14 days, this gene being involved in sensing stress signals and stimulating muscle hypertrophy (Kojic *et al.* 2004). The myostatin inhibitors caveolin-3 (*Cav3*) and follistatin (*Fst*) (Ohsawa *et al.* 2008; Lee, 2010) were up-regulated in response to passive loading at 5–8 and 9–14 days, respectively, suggesting a stimulation of muscle growth. Moreover, caveolin-3 expression increases during myofibre hypertrophy (Fanzani *et al.* 2007) and transgenic mice expressing the human isoform of follistatin display a dramatic increase in muscle mass (Lee & McPherron, 2001). It has been demonstrated that caveolin-3 interacts with neuronal nitric oxide synthase (nNOS) (North *et al.* 1993) and leads to the inhibition of nNOS activity. Suzuki *et al.* (2007) have shown that in hindlimb suspension, cytoplasmic translocation of nNOS regulates Foxo3a, MuRF-1 and Atrogin-1/MAFbx throughout nitric oxide (NO) production, leading to muscle atrophy. At the gene level, neuronal nitric oxide synthase 1 (*Nos1*) was down-regulated from 5 to 8 days in parallel with the up-regulation of *Cav3*, suggesting a down-regulation of upstream regulators of proteolysis pathways. Furthermore, *Cav3*, *Nos1* and *Ankrd2* are all important mechanosensors (Kojic *et al.* 2004; Llano-Diez *et al.* 2011), supporting their role in the intracellular signalling processes leading to the improved muscle size and function in response to loading in the mechanically silenced muscles in the experimental ICU model.

Regulation of stress response

It is well known that disuse and immobilization of skeletal muscles induce oxidative stress with increasing levels of reactive oxygen species (Dalla Libera *et al.* 2009; Powers *et al.* 2010). In accordance with this, an increased amount of carbonylated proteins was observed after long-term (9–14 days) exposure to immobilization in the ICU model and paralleled by an increased oxidative stress response at the gene level from 5 to 14 days (Llano-Diez *et al.* 2011). Passive loading, on the other hand, decreased the oxidative stress response from 5 to 14 days at the gene level and reduced the amount of carbonylated proteins. Grp94 is a calcium-binding chaperone of the

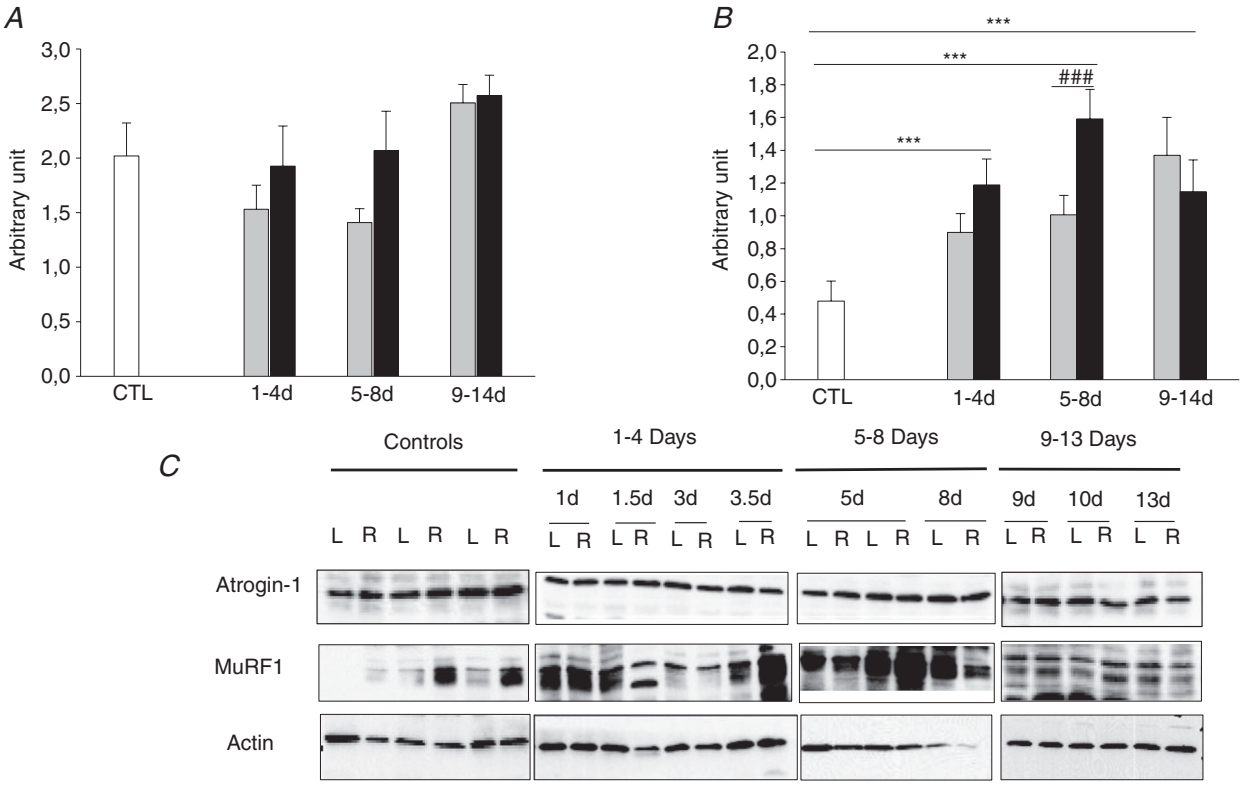

Figure 8. Western blots of Atrogin-1 and MuRF1 in the soleus muscle in response to unilateral mechanical loading
A and *B*, Western blot analyses of Atrogin-1 (*A*) and MuRF1 (*B*) in the soleus muscle normalized to actin contents in response to unilateral mechanical loading in rats exposed to NMB and mechanical ventilation at durations varying from 0 h (controls in white) to 14 days (loaded in grey and unloaded in black). Values are mean + SD. ***$P < 0.01$ (significant difference compared with controls); ###$P < 0.01$ (significant difference compared with unloaded).

endoplasmic reticulum involved in the maintenance of calcium homeostasis and in cytoprotection of muscle and neural cells against oxidative stress (Vitadello *et al.* 2003; Bando *et al.* 2004; Pizzo *et al.* 2010). Grp94 was up-regulated at the protein level in the loaded plantaris muscle compared with the unloaded side from 5 to 8 days, despite decreased accumulation of the respective mRNA. However, this apparent contradiction might explain the return of Grp94 levels to control values over the next few days. Alternatively, an increase of Grp94 protein levels might result from a general negative effect of passive loading on protein catabolism. Although these results suggest a rather complex regulation of Grp94 expression in ICU intervention, Grp94 protein levels appear to be influenced, at least in part, by muscle loading, being positively affected by passive loading, and negatively by muscle silencing (this manuscript) or by unweighting due to hindlimb suspension (L. Gorza *et al.*, unpublished data). At the cellular level, Grp94 is required for folding of insulin growth factor I (IGF-I) and IGF-II, the major positive autocrine regulators of muscle growth and regeneration (Yang *et al.* 1996; Pelosi *et al.* 2007; Ostrovsky *et al.* 2009, 2010). Whereas unloading does not appear to affect IGF mRNA levels (Heinemeier *et al.* 2009), here we show that passive loading increased growth factor transcripts. Conversely, lower levels of IGF-1 were observed in soleus muscles after hindlimb unloading (Suliman *et al.* 1999; Han *et al.* 2007), a condition where Grp94 levels were also significantly reduced (L. Gorza *et al.*, unpublished data). As reported during submission of the present work, conditional ablation of Grp94 in fetal skeletal muscle resulted in diminished skeletal muscle IGF production and significant loss in muscle mass, which could be rescued by systemic administration of recombinant IGF-I (Barton *et al.* 2012). Further, unpublished results from L. Gorza and co-workers demonstrate that recombinant Grp94 expression reduces both atrophy and oxidative stress in response to hindlimb suspension in transfected muscle fibres. Thus, the transient up-regulation of Grp94 in response to mechanical loading, the increase in carbonylated proteins on the unloaded side and the up-regulation of *Igf-2* in response to loading may accordingly represent important mechanisms involved in the sparing of mass and function in the mechanically loaded pharmacologically paralysed limb muscles.

Potential limitations and weaknesses

It may be questioned whether the experimental rat model used in this study resembles the ICU condition, as postsynaptic neuromuscular blockade and controlled mechanical ventilation is used less frequently in modern ICUs than in the past. However, in spite of less frequent use of NMB and controlled mechanical ventilation, AQM and a preferential myosin loss remain frequently observed among ICU patients. In previous experimental studies we have shown that the addition of NMB to mechanical ventilation and immobilization does not have a significant negative additive effect on single muscle fibre-specific force in an experimental porcine ICU model (Ochala *et al.* 2011*a*). Furthermore, we have recently shown that complete immobilization in deeply sedated and mechanically ventilated ICU patients induced the preferential myosin loss observed in patients with AQM in the absence of NMB (Llano-Diez *et al.* 2012). Thus, the mechanical silencing *per se*, absence of weight-bearing and internal strain caused by muscle contraction appears to play a dominant role in the preferential myosin loss observed in ICU patients with AQM and in experimental ICU models and being independent of NMB.

Significant effects on muscle fibre size and regulation of muscle contraction were observed in response to the unilateral loading. These effects were associated with significant changes in gene/protein expression, protein carbonylations, expression of the protein chaperone Grp94 and in the ubiquitin–proteasome proteolytic pathway. The signalling pathways involved in this *in vivo* model are very complex, involving multiple pathways. Detailed analyses of the signalling pathways involved in both the ICU muscle wasting *per se* as well as the effects of passive mechanical loading are both interesting and warranted, but beyond the scope of the present study.

Conclusions

Passive mechanical loading had a significant positive effect on limb muscle mass and function in animals exposed to ICU intervention, i.e. passive loading reduced the single muscle fibre atrophy and loss of specific force, resulting in a doubling of the functional capacity of the loaded *versus* the unloaded muscles after a 2 week ICU intervention. The improved maintenance of muscle mass and function in response to loading were associated with a reduced myosin loss, an increased transcriptional regulation of contractile proteins, a decreased oxidative stress revealed by lower levels of carbonylated proteins on the loaded *versus* the unloaded side and decreased activation of the ubiquitin–proteasome pathway. Thus, the results from this study show that passive mechanical loading alleviates the severe negative consequences on muscle size and function associated with the mechanical silencing in ICU patients, strongly supporting early and intense physical therapy in immobilized ICU patients.

References

Balagopal P, Ford GC, Ebenstein DB, Nadeau DA & Nair KS (1996). Mass spectrometric methods for determination of [^{13}C]leucine enrichment in human muscle protein. *Anal Biochem* **239**, 77–85.

Bando Y, Katayama T, Aleshin AN, Manabe T & Tohyama M (2004). GRP94 reduces cell death in SH-SY5Y cells perturbated calcium homeostasis. *Apoptosis* **9**, 501–508.

Barton ER, Park S, James JK, Makarewich CA, Philippou A, Eletto D, Lei H, Brisson B, Ostrovsky O, Li Z & Argon Y (2012). Deletion of muscle GRP94 impairs both muscle and body growth by inhibiting local IGF production. *FASEB J* **26**, 3691–3702.

Burns JR & Jones FL (1975). Letter: Early ambulation of patients requiring ventilatory assistance. *Chest* **68**, 608.

Burtin C, Clerckx B, Robbeets C, Ferdinande P, Langer D, Troosters T, Hermans G, Decramer M & Gosselink R (2009). Early exercise in critically ill patients enhances short-term functional recovery. *Crit Care Med* **37**, 2499–2505.

Chen YW, Zhao P, Borup R & Hoffman EP (2000). Expression profiling in the muscular dystrophies: identification of novel aspects of molecular pathophysiology. *J Cell Biol* **151**, 1321–1336.

Cheung AM, Tansey CM, Tomlinson G, Diaz-Granados N, Matte A, Barr A, Mehta S, Mazer CD, Guest CB, Stewart TE, Al-Saidi F, Cooper AB, Cook D, Slutsky AS & Herridge MS (2006). Two-year outcomes, health care use, and costs of survivors of acute respiratory distress syndrome. *Am J Respir Crit Care Med* **174**, 538–544.

Chong SM & Jin JP (2009). To investigate protein evolution by detecting suppressed epitope structures. *J Mol Evol* **68**, 448–460.

Dalla Libera L, Ravara B, Gobbo V, Tarricone E, Vitadello M, Biolo G, Vescovo G & Gorza L (2009). A transient antioxidant stress response accompanies the onset of disuse atrophy in human skeletal muscle. *J Appl Physiol* **107**, 549–557.

De Jonghe B, Sharshar T, Lefaucheur JP, Authier FJ, Durand-Zaleski I, Boussarsar M, Cerf C, Renaud E, Mesrati F, Carlet J, Raphael JC, Outin H & Bastuji-Garin S (2002). Paresis acquired in the intensive care unit: a prospective multicenter study. *JAMA* **288**, 2859–2867.

Dworkin BR & Dworkin S (1990). Learning of physiological responses: I. Habituation, sensitization, and classical conditioning. *Behav Neurosci* **104**, 298–319.

Dworkin BR & Dworkin S (2004). Baroreflexes of the rat. III. Open-loop gain and electroencephalographic arousal. *Am J Physiol Regul Integr Comp Physiol* **286**, R597–R605.

Essen P, McNurlan MA, Gamrin L, Hunter K, Calder G, Garlick PJ & Wernerman J (1998). Tissue protein synthesis rates in critically ill patients. *Crit Care Med* **26**, 92–100.

Fabiato A (1988). Computer programs for calculating total from specified free or free from specified total ionic concentrations in aqueous solutions containing multiple metals and ligands. *Methods Enzymol* **157**, 378–417.

Fanzani A, Musarò A, Stoppani E, Giuliani R, Colombo F, Preti A & Marchesini S (2007). Hypertrophy and atrophy inversely regulate Caveolin-3 expression in myoblasts. *Biochem Biophys Res Commun* **357**, 314–318.

Ford GC, Cheng KN & Halliday D (1985). Analysis of ($^{1-13}$C)leucine and (^{13}C)KIC in plasma by capillary gas chromatography/mass spectrometry in protein turnover studies. *Biomed Mass Spectrom* **12**, 432–436.

Frontera WR & Larsson L (1997). Contractile studies of single human skeletal muscle fibers: a comparison of different muscles, permeabilization procedures, and storage techniques. *Muscle Nerve* **20**, 948–952.

Gamrin L, Essen P, Hultman E, McNurlan MA, Garlick PJ & Wernerman J (2000). Protein-sparing effect in skeletal muscle of growth hormone treatment in critically ill patients. *Ann Surg* **231**, 577–586.

Grefte S, Kuijpers-Jagtman AM, Torensma R & Von den Hoff JW (2007). Skeletal muscle development and regeneration. *Stem Cells Dev* **16**, 857–868.

Grune T, Merker K, Sandig G & Davies KJ (2003). Selective degradation of oxidatively modified protein substrates by the proteasome. *Biochem Biophys Res Commun* **305**, 709–718.

Han B, Zhu MJ, Ma C & Du M (2007). Rat hindlimb unloading down-regulates insulin like growth factor-1 signaling and AMP-activated protein kinase, and leads to severe atrophy of the soleus muscle. *Appl Physiol Nutr Metab* **32**, 1115–1123.

Heinemeier KM, Olesen JL, Haddad F, Schjerling P, Baldwin KM & Kjaer M (2009). Effect of unloading followed by reloading on expression of collagen and related growth factors in rat tendon and muscle. *J Appl Physiol* **106**, 178–186.

Herridge MS (2011). Recovery and long-term outcome in acute respiratory distress syndrome. *Crit Care Clin* **27**, 685–704.

Herridge MS, Cheung AM, Tansey CM, Matte-Martyn A, Diaz-Granados N, Al-Saidi F, Cooper AB, Guest CB, Mazer CD, Mehta S, Stewart TE, Barr A, Cook D & Slutsky AS (2003). One-year outcomes in survivors of the acute respiratory distress syndrome. *N Engl J Med* **348**, 683–693.

Herridge MS, Tansey CM, Matte A, Tomlinson G, Diaz-Granados N, Cooper A, Guest CB, Mazer CD, Mehta S, Stewart TE, Kudlow P, Cook D, Slutsky AS & Cheung AM (2011). Functional disability 5 years after acute respiratory distress syndrome. *N Engl J Med* **364**, 1293–1304.

Huang da W, Sherman BT, Tan Q, Collins JR, Alvord WG, Roayaei J, Stephens R, Baseler MW, Lane HC & Lempicki RA (2007). The DAVID Gene Functional Classification Tool: a novel biological module-centric algorithm to functionally analyze large gene lists. *Genome Biol* **8**, R183.

Irizarry RA, Hobbs B, Collin F, Beazer-Barclay YD, Antonellis KJ, Scherf U & Speed TP (2003). Exploration, normalization, and summaries of high density oligonucleotide array probe level data. *Biostatistics* **4**, 249–264.

Jin JP, Yang FW, Yu ZB, Ruse CI, Bond M & Chen A (2001). The highly conserved COOH terminus of troponin I forms a Ca^{2+}-modulated allosteric domain in the troponin complex. *Biochemistry* **40**, 2623–2631.

Kojic S, Medeot E, Guccione E, Krmac H, Zara I, Martinelli V, Valle G & Faulkner G (2004). The Ankrd2 protein, a link between the sarcomere and the nucleus in skeletal muscle. *J Mol Biol* **339**, 313–325.

Larsson L (2008). Acute quadriplegic myopathy: an acquired "myosinopathy". *Adv Exp Med Biol* **642**, 92–98.

Larsson L & Moss RL (1993). Maximum velocity of shortening in relation to myosin isoform composition in single fibres from human skeletal muscles. *J Physiol* **472**, 595–614.

Lee SJ (2010). Extracellular regulation of myostatin: a molecular rheostat for muscle mass. *Immunol Endocr Metab Agents Med Chem* **10**, 183–194.

Lee SJ & McPherron AC (2001). Regulation of myostatin activity and muscle growth. *Proc Natl Acad Sci U S A* **98**, 9306–9311.

Leijten FS, Harinck-de Weerd JE, Poortvliet DC & de Weerd AW (1995). The role of polyneuropathy in motor convalescence after prolonged mechanical ventilation. *JAMA* **274**, 1221–1225.

Lewis SE, Kelly FJ & Goldspink DF (1984). Pre- and post-natal growth and protein turnover in smooth muscle, heart and slow- and fast-twitch skeletal muscles of the rat. *Biochem J* **217**, 517–526.

Li C & Wong WH (2001). Model-based analysis of oligonucleotide arrays: expression index computation and outlier detection. *Proc Natl Acad Sci U S A* **98**, 31–36.

Ljungqvist OH, Persson M, Ford GC & Nair KS (1997). Functional heterogeneity of leucine pools in human skeletal muscle. *Am J Physiol* **273**, E564–E570.

Llano-Diez M, Gustafson AM, Olsson C, Goransson H & Larsson L (2011). Muscle wasting and the temporal gene expression pattern in a novel rat intensive care unit model. *BMC Genomics* **12**, 602.

Llano-Diez M, Renaud G, Andersson M, Gonzales Marrero H, Cacciani N, Engquist H, Corpeno R, Artemenko K, Bergquist J & Larsson L (2012). Mechanisms underlying intensive care unit muscle wasting and effects of passive mechanical loading. *Crit Care* **16**, R209.

Martin UJ, Hincapie L, Nimchuk M, Gaughan J & Criner GJ (2005). Impact of whole-body rehabilitation in patients receiving chronic mechanical ventilation. *Crit Care Med* **33**, 2259–2265.

Metges CC, Petzke KJ & Hennig U (1996). Gas chromatography/combustion/isotope ratio mass spectrometric comparison of N-acetyl- and N-pivaloyl amino acid esters to measure ^{15}N isotopic abundances in physiological samples: a pilot study on amino acid synthesis in the upper gastro-intestinal tract of minipigs. *J Mass Spectrom* **31**, 367–376.

Morris PE, Goad A, Thompson C, Taylor K, Harry B, Passmore L, Ross A, Anderson L, Baker S, Sanchez M, Penley L, Howard A, Dixon L, Leach S, Small R, Hite RD & Haponik E (2008). Early intensive care unit mobility therapy in the treatment of acute respiratory failure. *Crit Care Med* **36**, 2238–2243.

Moss RL (1979). Sarcomere length–tension relations of frog skinned muscle fibres during calcium activation at short lengths. *J Physiol* **292**, 177–192.

Nava S (1998). Rehabilitation of patients admitted to a respiratory intensive care unit. *Arch Phys Med Rehabil* **79**, 849–854.

Nordquist J, Höglund A, Norman H, Tang X, Dworkin B & Larsson L (2007). Transcription factors in muscle atrophy caused by blocked neuromuscular transmission and muscle unloading in rats. *Mol Med* **13**, 461–470.

Norman H, Nordquist J, Andersson P, Ansved T, Tang X, Dworkin B & Larsson L (2006). Impact of post-synaptic block of neuromuscular transmission, muscle unloading and mechanical ventilation on skeletal muscle protein and mRNA expression. *Pflugers Arch* **453**, 53–66.

North AJ, Galazkiewicz B, Byers TJ, Glenney JR, Jr & Small JV (1993). Complementary distributions of vinculin and dystrophin define two distinct sarcolemma domains in smooth muscle. *J Cell Biol* **120**, 1159–1167.

Ochala J, Ahlbeck K, Radell PJ, Eriksson LI & Larsson L (2011*a*). Factors underlying the early limb muscle weakness in acute quadriplegic myopathy using an experimental ICU porcine model. *PLoS One* **6**, e20876.

Ochala J, Gustafson AM, Diez ML, Renaud G, Li M, Aare S, Qaisar R, Banduseela VC, Hedstrom Y, Tang X, Dworkin B, Ford GC, Nair KS, Perera S, Gautel M & Larsson L (2011*b*). Preferential skeletal muscle myosin loss in response to mechanical silencing in a novel rat intensive care unit model: underlying mechanisms. *J Physiol* **589**, 2007–2026.

Ochala J, Renaud G, Llano Diez M, Banduseela VC, Aare S, Ahlbeck K, Radell PJ, Eriksson LI & Larsson L (2011*c*). Diaphragm muscle weakness in an experimental porcine intensive care unit model. *PLoS One* **6**, e20558.

Ohsawa Y, Okada T, Kuga A, Hayashi S, Murakami T, Tsuchida K, Noji S & Sunada Y (2008). Caveolin-3 regulates myostatin signaling. Mini-review. *Acta Myol* **27**, 19–24.

Ostrovsky O, Ahmed NT & Argon Y (2009). The chaperone activity of GRP94 toward insulin-like growth factor II is necessary for the stress response to serum deprivation. *Mol Biol Cell* **20**, 1855–1864.

Ostrovsky O, Eletto D, Makarewich C, Barton ER & Argon Y (2010). Glucose regulated protein 94 is required for muscle differentiation through its control of the autocrine production of insulin-like growth factors. *Biochim Biophys Acta* **1803**, 333–341.

Pelosi L, Giacinti C, Nardis C, Borsellino G, Rizzuto E, Nicoletti C, Wannenes F, Battistini L, Rosenthal N, Molinaro M & Musaro A (2007). Local expression of IGF-1 accelerates muscle regeneration by rapidly modulating inflammatory cytokines and chemokines. *FASEB J* **21**, 1393–1402.

Pizzo P, Scapin C, Vitadello M, Florean C & Gorza L (2010). Grp94 acts as a mediator of curcumin-induced antioxidant defence in myogenic cells. *J Cell Mol Med* **14**, 970–981.

Powers S, Duarte J, Kavazis A & Talbert E (2010). Reactive oxygen species are signalling molecules for skeletal muscle adaptation. *Exp Physiol* **95**, 1–9.

Raskin AM, Hoshijima M, Swanson E, McCulloch AD & Omens JH (2009). Hypertrophic gene expression induced by chronic stretch of excised mouse heart muscle. *Mol Cell Biomech* **6**, 145–159.

Ross G (1972). A method for augmenting ventilation during ambulation. *Phys Ther* **52**, 519–520.

Smyth GK (2004). Linear models and empirical Bayes methods for assessing differential expression in microarray experiments. *Stat Appl Genet Mol Biol* **3**, Article 3.

Suliman IA, Lindgren JU, Gillberg PG, Elhassan AM, Monneron C & Adem A (1999). Alteration of spinal cord IGF-I receptors and skeletal muscle IGF-I after hind-limb immobilization in the rat. *Neuroreport* **10**, 1195–1199.

Suzuki N, Motohashi N, Uezumi A, Fukada S, Yoshimura T, Itoyama Y, Aoki M, Miyagoe-Suzuki Y & Takeda S (2007). NO production results in suspension-induced muscle

atrophy through dislocation of neuronal NOS. *J Clin Invest* **117**, 2468–2476.

Tjader I, Rooyackers O, Forsberg AM, Vesali RF, Garlick PJ & Wernerman J (2004). Effects on skeletal muscle of intravenous glutamine supplementation to ICU patients. *Intensive Care Med* **30**, 266–275.

Vitadello M, Penzo D, Petronilli V, Michieli G, Gomirato S, Menabo R, Di Lisa F & Gorza L (2003). Overexpression of the stress protein Grp94 reduces cardiomyocyte necrosis due to calcium overload and simulated ischemia. *FASEB J* **17**, 923–925.

Yang CQ, Zhan X, Hu X, Kondepudi A & Perdue JF (1996). The expression and characterization of human recombinant proinsulin-like growth factor II and a mutant that is defective in the O-glycosylation of its E domain. *Endocrinology* **137**, 2766–2773.

Authors contributions

The experimental work was performed in the research laboratory of L.L. in the Department of Neuroscience, Clinical Neurophysiology, Uppsala University. with the assistance of N.C., A.-M.G., Y.H., M.L.-D. and G.R. Microarray analysis were performed by M.L.-D. Protein expression analyses were performed by B.R., R.C., A.-M.G., Y.H., G.R., H.-Z.F. and B.R. Single fibre contractile recordings were performed by J.O. and G.R. Fractional protein synthesis rate analyses were performed by G.C.F. and S.N. Protein carbonylation and Grp94 analyses were performed by B.R. and L.G. Filament analyses were performed by H.-Z.F. and J.-P.J. L.L. initiated/designed the experiments and wrote the manuscript with assistance from G.R., M.L.-D., S.N., J.P.G. and L.G. All authors approved the final version of the manuscript. The authors declare no conflict of interest.

Acknowledgements

This study was supported by grants from the Swedish Research Council (8651), STINT, King Gustaf V Research Foundation, the European Commission (MyoAge, EC Fp7 CT-223756 and COST CM1001), Uppsala University and Uppsala University Hospital, to L.L. and ASI-OSMA (WP1B51-2) to L.G.